Anisotropy analysis of third-harmonic generation in a germanium-doped silica optical fiber

Adrien Borne,[1] Tomotaka Katsura,[2] Corinne Félix,[1] Benjamin Doppagne,[1] Patricia Segonds,[1] Kamel Bencheikh,[3] Juan Ariel Levenson,[3] and Benoît Boulanger[1,*]

[1]*Institut Néel, CNRS/Université Joseph Fourier, BP 166, 38402 Grenoble, France*

[2]*Advanced Technology R&D Center, Mitsubishi Electric Corporation, 8-1-1, Tsukaguchi-honmachi, Amagasaki, Hyogo, Japan*

[3]*Laboratoire de Photonique et de Nanostructures, CNRS, Route de Nozay, 91460 Marcoussis, France*

**Corresponding author: benoit.boulanger@neel.cnrs.fr*

Received October 10, 2014; revised January 16, 2015; accepted January 20, 2015;
posted January 21, 2015 (Doc. ID 224337); published March 10, 2015

We performed an intermodal third-harmonic generation around 516 nm in a germanium-doped silica optical fiber. The analysis of the complex polarization behavior that was observed allowed us to determine the orientation symmetry group of the fiber and the relative values of the independent coefficients of the third-order electric susceptibility tensor. © 2015 Optical Society of America

OCIS codes: (190.4370) Nonlinear optics, fibers; (190.4410) Nonlinear optics, parametric processes; (190.2620) Harmonic generation and mixing.

http://dx.doi.org/10.1364/OL.40.000982

Birefringence in optical fibers has been extensively investigated. It can be an unwanted intrinsic property leading to undesirable effects that have to be suppressed. It can also be exploited as in the case of cross-phase modulation, for example where the birefringence influences the spectrum and leads to instability behaviors [1]. In polarization-maintaining fibers, the birefringence is well controlled and has led to numerous crucial applications, as in telecommunication [2]. In the present Letter, we report on the effects of a weak anisotropy in an optical fiber due to manufacture imperfection at the level of its birefringence as well as of its third-order electric susceptibility tensor. We performed that work in the case of third-harmonic generation (THG: $\omega + \omega + \omega \rightarrow 3\omega$) in a germanium-doped silica optical fiber enabling intermodal phase matching for a fundamental wavelength around 1550 nm. It comes in the context of the preparation of experiments of triple photon generation (TPG: $3\omega \rightarrow \omega + \omega + \omega$), which is one of the most tricky and challenging topics in nonlinear and quantum optics [3,4]. Due to the extreme weakness of the efficiency of the TPG, it is relevant to study the THG in a first step since these two processes have the same phase-matching properties [5]. We evidenced a complex polarization behavior of the THG that allowed us to determine the symmetry of the third-order electric susceptibility tensor of the studied fiber and the optimal configuration of polarization.

We used a silica fiber with a core radius of 2.19 μm and doped with a molar concentration of 37% of GeO_2 at its center. There is a parabolic gradient of concentration leading to an estimated average value of 28.2% over the core. The fiber was cleaved with a diamond tip Corning cleaver, perpendicularly to its axis. The corresponding core/cladding index difference is of about $\Delta n = 6 \times 10^{-2}$. The fiber was placed on a Thorlabs Nanomax three-axes stage of 1-μm step. We used 183-mm- and 642-mm-long fibers according to the performed studies. The two fibers were maintained uncoiled during the experiments. They were pumped by a beam emitted by a 10-Hz-repetition rate Panther optical parametric oscillator (OPO) with a pulse duration of 5 ns (FWHM), and tunable between 410 and 2400 nm in order to determine at best the THG phase-matching wavelength. The input fundamental power was measured by an OPHIR PE10 powermeter. At the output of the fiber, the fundamental and third-harmonic powers were measured using calibrated DET410 InGaAs and DET110 Si-based Thorlabs photodiodes, respectively. The experimental setup is described in Fig. 1. In the assumption of weak guiding, THG phase-matching is predicted when the fundamental field is in the LP_{01} mode (the fundamental Gaussian mode), while the third-harmonic one is in the LP_{03} mode [5]. We experimentally observed the right modal configuration, as shown in Fig. 2. Since the experimental LP_{03} mode exhibits a small ellipticity, of about 0.5, it is compared with a calculation performed in the elliptical Ince basis [6].

The fundamental phase-matching wavelength was found at 1550 nm very close to the calculation as shown in Fig. 3. The corresponding full width at half-maximum (FWHM) spectral acceptance is $L \cdot \delta\lambda_\omega = 120\ \text{nm} \cdot \text{cm}$, where L is the fiber length; the acceptance is mainly

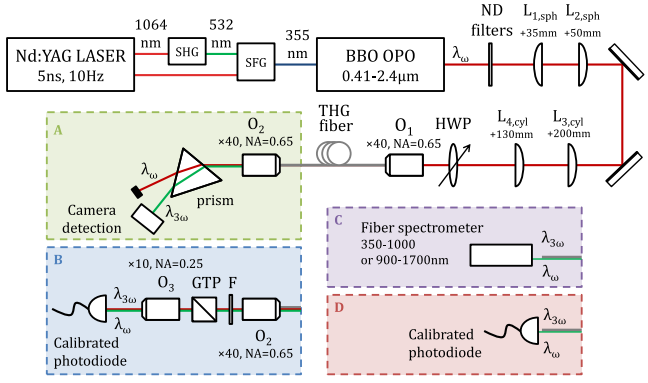

Fig. 1. Experimental setup used for the THG study: ND stands for neutral density, L for lens, HWP for half-wave plate, O_i for microscope objective, F for dichroic filters and GTP for Glan–Taylor polarizer; the different units are used for specific measurements: A for the modes imaging, B for the polarization configuration, C for the spectral properties, and D for the conversion efficiency.

 © 2015 Optical Society of America

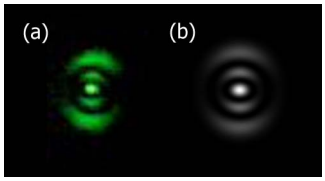

Fig. 2. Measured (a) and calculated (b) transverse distributions of the third-harmonic LP_{03} mode propagating in the 183-mm-long fiber at 516 nm.

governed by core size fluctuations: the agreement is reached for a fitting value of core radius fluctuations of 12 nm as shown in Fig. 3, which is in accordance with the fiber specifications. The peak of the calculated curve does not exhibit secondary maxima since it is the convolution of many sinc^2 functions at different core radii. Note that the calculated acceptance without any core fluctuation would be $L \cdot \delta\lambda_\omega = 1.5\ \mathrm{nm} \cdot \mathrm{cm}$ (FWHM). Figure 4 shows that the energy of the third-harmonic energy behaves cubically with the fundamental energy, reaching a maximum value of 43.8 fJ (810 $\mathrm{mW\,cm^{-2}}$) when the fundamental energy is equal to 0.58 μJ (6.25 $\mathrm{MW\,cm^{-2}}$). Although the fiber is 642 mm long, the THG conversion efficiency is very low due to the weakness of the incident power, which had the advantage of limiting the level of the parasitic effects that can occur in an optical fiber. The measurements and calculations of the modal configuration (cf. Fig. 2) as well as of the behavior of the third-harmonic energy as a function of the fundamental wavelength (cf. Fig. 3) and energy (cf. Fig. 4) clearly demonstrate that a phase-matched third-harmonic generation is well achieved in the optical fiber.

We then analyzed the polarization state of both the fundamental and third-harmonic waves at the exit of the fiber for different orientations of the linear polarization of the fundamental wave. Measurements are done in the experimental configuration B of Fig. 1. A half-wave plate controls the polarization of the incoming fundamental beam. The fundamental and third-harmonic beams are collected in a microscope objective. They can be considered separately using appropriate filters, and a Glan–Taylor polarizer allowed us to analyze their polarization state.

In a first step, we studied the fundamental beam only by putting the fiber between parallel or orthogonal

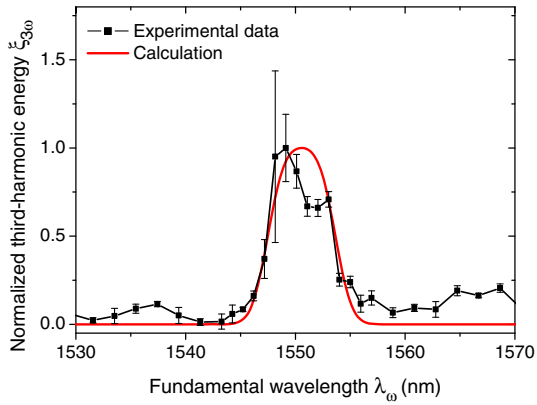

Fig. 3. Third-harmonic energy generated in the 183-mm-long fiber as a function of the fundamental energy around phase matching.

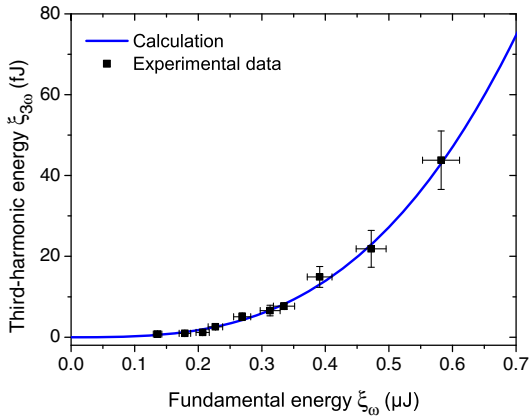

Fig. 4. Third-harmonic energy generated in the 642-mm-long fiber as a function of the fundamental energy.

polarizers. It is a standard technique of measurement widely used in crystal optics [7]. The half-wave plate and Glan–Taylor polarizer are then rotated together, and the transmitted energy is measured as a function of the rotation angle α, the fiber being kept fixed. The result is given in Fig. 5 for the parallel configuration. We saw a clear evidence of the anisotropy of the fiber, two successive maxima corresponding to the two orthogonal neutral lines. Note that the curve of Fig. 5 would be a horizontal line in the case of an isotropic medium. We assumed that the relevant optical class of the fiber is the uniaxial one, and we will see later on that it is a correct assumption. The propagation axis of the fiber being identified as exhibiting an anisotropy, it is necessarily an axis perpendicular to the optical axis of the uniaxial medium, which is named the z axis by the standard convention [7]. We arbitrarily called the fiber axis x, the cleaving plane being then the (yOz) plane. The axis at 0° in Fig. 5 is arbitrarily taken as the z axis, while the axis at 90° is the y axis.

In a second step, we analyzed the polarization of the third-harmonic wave as a function of the polarization of the fundamental wave. The result is given in Fig. 6. The analysis of this complex polarization behavior allowed us to determine the orientation symmetry of the fiber and thus the anisotropy of the third-order electric

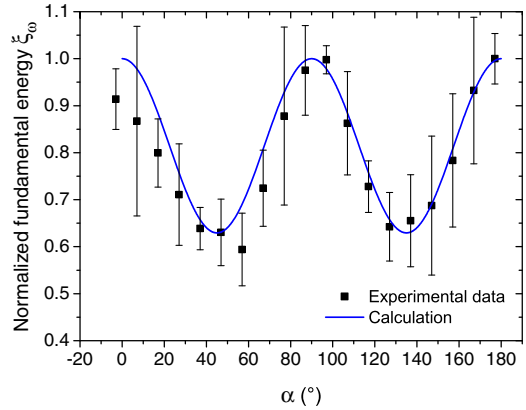

Fig. 5. Fundamental energy ξ_ω transmitted by the 642-mm-long fiber placed between parallel polarizer (half-wave plate) and analyzer (Glan–Taylor prism). α is the corresponding rotation angle of polarization.

susceptibility tensor. As the experiments were performed with an uncoiled fiber, the anisotropy cannot arise from the bends as it is usually the case in the standard use of an optical fiber. We assume that the mechanical stress has an intrinsic origin as a slight ellipticity of the core for example. We then assumed that the fiber belongs to the infinite group $\{A\infty/m, \infty m\}$, which corresponds to the case of an isotropic medium under an uniaxial strain, the $A\infty$ axis being the axis of the intrinsic stress. Under the Kleinman assumption, the corresponding nonzero independent coefficients of the third-order electric susceptibility tensor are the following [8]: $\chi_{xxxx} = \chi_{yyyy} = 3\chi_{xxyy} = 3\chi_{xyxy} = 3\chi_{yxxy} = 3\chi_{yxyx} = 3\chi_{yyxx} = 3\chi_{xyyx}$; χ_{zzzz}; $\chi_{xxzz} = \chi_{xzxz} = \chi_{zxxz} = \chi_{zxzx} = \chi_{zzxx} = \chi_{xzzx} = \chi_{yyzz} = \chi_{yzyz} = \chi_{zyyz} = \chi_{zyzy} = \chi_{zzyy} = \chi_{yzzy}$, where x, y and z are defined above. Thus, there are only three independent coefficients. Note that there is only one independent coefficient in the case of an isotropic medium, and the corresponding behavior of Fig. 6 would be an unique horizontal line. We considered all the possible configurations for which the effective coefficient is not nil, i.e., in terms of ordinary (o) and extraordinary (e) waves: $C_1(3\omega_o, \omega_o, \omega_o, \omega_o)$, $C_2(3\omega_e, \omega_e, \omega_e, \omega_e)$, $D_1(3\omega_o, \omega_o, \omega_e, \omega_e)$, $D_2(3\omega_e, \omega_e, \omega_o, \omega_o)$; configurations D_1 and D_2 have three equivalents each, which is due to the permutation over the three fundamental waves. The corresponding effective coefficients are respectively:

$$\begin{aligned}
\chi_{\text{eff}}^{C_1}(\theta_\omega^{\text{in}}) &= \chi_{yyyy}(3\omega)\sin^3(\theta_\omega^{\text{in}})e_{3\omega}^{y} \\
\chi_{\text{eff}}^{C_2}(\theta_\omega^{\text{in}}) &= \chi_{zzzz}(3\omega)\cos^3(\theta_\omega^{\text{in}})e_{3\omega}^{z} \\
\chi_{\text{eff}}^{D_1}(\theta_\omega^{\text{in}}) &= 3\chi_{yyzz}(3\omega)\cos(\theta_\omega^{\text{in}})\sin^2(\theta_\omega^{\text{in}})e_{3\omega}^{y} \\
\chi_{\text{eff}}^{D_2}(\theta_\omega^{\text{in}}) &= 3\chi_{yyzz}(3\omega)\sin(\theta_\omega^{\text{in}})\cos^2(\theta_\omega^{\text{in}})e_{3\omega}^{z}, \qquad (1)
\end{aligned}$$

where $\theta_\omega^{\text{in}}$ is the polarization angle of the fundamental wave relative to the z axis, while $e_{3\omega}^{y}$ and $e_{3\omega}^{z}$ are the Cartesian coordinates of the third-harmonic unit electric field vector along the y axis and z axis, respectively. The third-harmonic phase-matching wavelengths corresponding to the different combinations of polarization range from 516.4 nm for $\theta_\omega^{\text{in}} = 90°$ (C_1 configuration only) and 516.9 nm for $\theta_\omega^{\text{in}} = 0°$ (C_2 configuration only) according to spectral measurements. This slight difference of wavelength is one order of magnitude lower than the linewidth of the fundamental beam, i.e., 4.9 nm around 1.6 μm, so that the calculation of the overall generated energy of the third-order harmonic wave can be done assuming that all the possible processes are at the same wavelength. But this difference of wavelengths can be also used for an estimate of the birefringence by assuming that the dispersion of the refractive index can be neglected from 516.4 and 516.9 nm. Hence we find: $[n_y(\text{LP}_{03}) - n_z(\text{LP}_{03})] = 9 \times 10^{-5}$, which is weak as expected. We calculated the corresponding third-harmonic power density transmitted by the analyzer as a function of the fundamental polarization angle $\theta_\omega^{\text{in}}$ and of the analyzer angle θ_A relative to the z axis. Because the efficiency of interaction is very low, the undepleted pump approximation can be assumed, so that $I_{3\omega}^{\text{out}}$ can be obtained by summing the intensities of the four processes described by Eqs. 1 taken independently, which gives:

$$I_{3\omega}^{\text{out}}(\theta_\omega^{\text{in}}, \theta_A) \propto \Gamma_1(\theta_\omega^{\text{in}})\sin^2(\theta_A) + \Gamma_2(\theta_\omega^{\text{in}})\cos^2(\theta_A), \qquad (2)$$

where

$$\Gamma_i(\theta_\omega^{\text{in}}) = [\chi_{\text{eff}}^{C_i}(\theta_\omega^{\text{in}})]^2 + [\chi_{\text{eff}}^{D_i}(\theta_\omega^{\text{in}})]^2, \qquad (3)$$

with $i \in \{1, 2\}$. Since it is not possible to access any other direction of propagation than that corresponding to the fiber axis, i.e., the x axis of the dielectric frame defined above, it is not possible to determine the magnitudes of the different elements of the third-order electric susceptibility tensor of the fiber as it can be done in the case of any bulk crystal. But from Fig. 6, we showed that it is possible to access the magnitude of the following ratios that characterize the anisotropy of the third-order electric susceptibility tensor: $\Psi = \chi_{yyyy}/\chi_{zzzz}$, and $\Omega = \chi_{yyzz}/\chi_{zzzz}$. For determining Ψ and Ω, and in order to reduce the uncertainty of the measurements, we considered the third-harmonic intensity integrated over the analyzer angle θ_A from 0 to 2π, namely $I_{3\omega}^{\text{tot}}$, which corresponds to the full intensity that would be generated inside the fiber. Then from Eqs. (1)–(3), it comes:

$$\begin{aligned}
I_{3\omega}^{\text{tot}}(\theta_\omega^{\text{in}}) \propto\ & [\chi_{yyyy}]^2\sin^6(\theta_\omega^{\text{in}}) + [\chi_{zzzz}]^2\cos^6(\theta_\omega^{\text{in}}) \\
& + \frac{9}{4}[\chi_{yyzz}]^2\sin^2(2\theta_\omega^{\text{in}}). \qquad (4)
\end{aligned}$$

From Eqs. (4), it is easy to bring up the coefficients Ψ and Ω by considering the ratio between the values of the total third-harmonic intensity at two different angles, namely $\theta_\omega^{\text{in}}$ and $\tilde{\theta}_\omega^{\text{in}}$, of the incident fundamental polarization, which gives:

$$\frac{I_{3\omega}^{\text{tot}}(\theta_\omega^{\text{in}})}{I_{3\omega}^{\text{tot}}(\tilde{\theta}_\omega^{\text{in}})} = \frac{\Psi^2\sin^6(\theta_\omega^{\text{in}}) + \cos^6(\theta_\omega^{\text{in}}) + \frac{9}{4}\Omega^2\sin^2(2\theta_\omega^{\text{in}})}{\Psi^2\sin^6(\tilde{\theta}_\omega^{\text{in}}) + \cos^6(\tilde{\theta}_\omega^{\text{in}}) + \frac{9}{4}\Omega^2\sin^2(2\tilde{\theta}_\omega^{\text{in}})}. \qquad (5)$$

Then according to the ratio given by Eq. (5), the different pairs of experimental curves of Fig. 6 led to the determination of the two unknown coefficients Ψ and Ω. In order to get the best accuracy, we considered fit angles for which the weights of the three coefficients

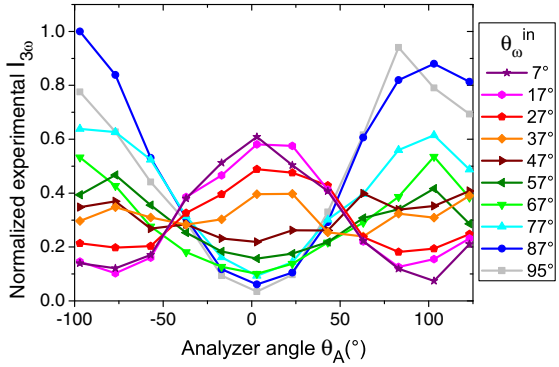

Fig. 6. Normalized measured third-harmonic energy generated in the 642-mm-long fiber plotted as a function of the analyzer angle θ_A for different values $\theta_\omega^{\text{in}}$ of the input linearly polarized fundamental wave. The error bars of the measurements are not put for more clarity; the corresponding uncertainty is of about ±5.5%.

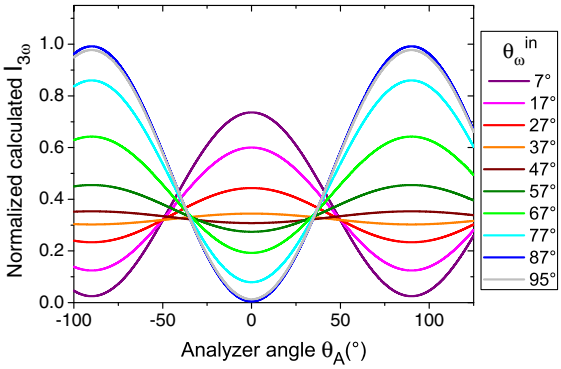

Fig. 7. Normalized calculated third-harmonic energy generated in the 642-mm-long fiber plotted as a function of the analyzer angle θ_A for different values $\theta_\omega^{\text{in}}$ of the input linearly polarized fundamental wave.

are close to each other. For example, from $(\theta_\omega^{\text{in}}, \tilde{\theta}_\omega^{\text{in}}) = (47°, 17°)$ and $(95°, 17°)$, it comes $I_{3\omega}^{\text{tot}}(\theta_\omega^{\text{in}})/I_{3\omega}^{\text{tot}}(\tilde{\theta}_\omega^{\text{in}}) = 0.91$ and 1.37, respectively, leading to: $\Psi = 1.14 \pm 0.02$ and $\Omega = 0.50 \pm 0.02$; it implies that $\chi_{yyzz} < \chi_{zzzz} < \chi_{yyyy}$. This result is strongly corroborated by the relation of order at the level of the refractive indices, since we had found $n_z < n_y$. Note that this way of proceeding is validated by the fact that these particular values of Ψ and Ω lead to a perfect calculation at any angle. From the magnitudes of Ψ and Ω, it is then easy to calculate the normalized third-harmonic intensity from Eqs. (1) to (3). Figure 7 gives the result for the same angles of polarization of the fundamental wave than those taken for the measurements of Fig. 6 for a direct comparison. There is a remarkable agreement between measurements and calculations, which fully validates our hypothesis of an uniaxial fiber belonging to the $\{A\infty/m, \infty m\}$ group on one hand, and the relative values of the independent coefficients of the third-order electric susceptibility tensor of the fiber on the other hand. From the values of Ψ and Ω that were determined, and the measurement of the absolute value of one of the three unknown tensor coefficients, χ_{yyyy}, χ_{yyzz} or χ_{zzzz}, it would be possible to determine the absolute value of the two other coefficients. It was not done in the present work since it would not have been possible to access the effective interaction area of the nonlinear interaction with a sufficient accuracy [9].

As a conclusion, we performed modal, spectral, energetic, and polarization characterizations of intermodal THG ($LP_{01,\omega} \rightarrow LP_{03,3\omega}$) in a germanium-doped silica optical fiber. We evidenced and accurately modeled for the first time to the best of our knowledge the polarization behavior involving all the possible phase-matching types that simultaneously occur in a weakly anisotropic optical fiber. Calculations are in strong agreement with experiments. These measurements will allow us to prepare at best spontaneous TPG experiments, i.e., the emblematic third-order parametric fluorescence, in particular with respect to polarization entanglement aspects.

The authors gratefully acknowledge DRAKA, which provided the optical fibers.

References

1. G. Millot, E. Seve, S. Wabnitz, and M. Haelterman, J. Opt. Soc. Am. B **15**, 1266 (1998).
2. See for example P. Drexler and P. Fiala, *Optical Fiber Birefringence Effects: Sources, Utilization and Methods of Suppression*, *Recent Progress in Optical Fiber Research*, M. Yasin, ed. (InTech, 2012).
3. M. Corona, K. Garay-Palmett, and A. B. U'Ren, Phys. Rev. Lett. **36**, 190 (2011).
4. S. Richard, K. Bencheikh, B. Boulanger, and J. A. Levenson, Opt. Lett. **36**, 3000 (2011).
5. K. Bencheikh, S. Richard, G. Mélin, G. Krabshuis, F. Gooijer, and J. A. Levenson, Opt. Lett. **37**, 289 (2012).
6. M. A. Bandres and J. Gutiérrez-Vega, Opt. Lett. **29**, 144 (2004).
7. J. F. Nye, *Physical Properties of Crystals* (Clarendon, 1985).
8. P. N. Butcher and D. Cotter, *Cambridge Series in Modern Optics* (Cambridge University, 1990).
9. G. Agrawal, *Nonlinear Fiber Optics* (Academic, 2013).